INTERNATIONAL JOURNAL FOR NUMERICAL METHODS IN FLUIDS, VOL. 17, 1097–1114 (1993)

A PROPOSED THROUGH-FLOW INVERSE METHOD FOR THE DESIGN OF MIXED-FLOW PUMPS

JOÃO EDUARDO BORGES

Mechanical Engineering Department, Instituto Superior Técnico, Av. Rovisco Pais, 1096 Lisboa Codex, Portugal

SUMMARY

A through-flow (hub-to-shroud) truly inverse method is proposed and described in this paper. It uses as a initial design specification, an imposition of mean swirl, i.e. radius times mean tangential velocity, given throughout the meridional section of the turbomachine. In the present implementation, it is assumed that the fluid is invsicid, incompressible and irrotational at inlet and the blades are supposed to have zero thickness. Only blade rows that impart to the fluid a constant work along the span will be considered.

An application of this procedure to design the rotor of a mixed-flow pump will be described in detail. The strategy used to find a suitable mean swirl distribution and the other design inputs is also described. The final blade shape and pressure distributions on the blade surface are presented, showing that it is possible to obtain feasible designs using this technique. Another advantage of this technique is the fact that it does not require large amounts of CPU time.

KEY WORDS Inverse problems Turbomachinery Mixed-flow pumps Through-flow methods

1. INTRODUCTION AND LITERATURE SURVEY

A large majority of pumps are designed by using very simple and rudimentary one-dimensional considerations concerning the velocity triangles, which allow the calculation of the evolution of the blade angle along the passage, see, e.g. References 1 and 2. These methods are so easy that they can be carried out using only hand calculations and simple graphical processes.

Althouth some pumps are still being calculated using hand calculations, the above one-dimensional procedure can and has been programmed as computer codes which are being used by the most important pump manufacturers. The more radial the blade passage is, the better are the results obtained with these techniques. However, for mixed-flow pumps, the velocity triangles vary appreciably along the span, so that the above methodology is not good enough. In order to take into account this effect in some way, designers usually split the flow passage in several channels along the span, applying the above considerations to each one.

When the pump designs involve some responsibility, the above step is followed by a verification using a direct code which is run with the geometry arrived at previously. Before reaching the final design, several iterations following the above steps are usually required.

This complete process can be time-consuming, so that one is left wondering whether it could be improved. One possible way to achieve this could be by using inverse methods, enabling the achievement of the blade row layout in a more direct form, in one single step. Among inverse methods, two-dimensional techniques are the most frequently used and the ones that require less CPU time. These two-dimensional inverse methods can be classified into two main groups,

0271–2091/93/241097–18$14.00

Received August 1992
Revised August 1993

according to the approximations used when looking for the solution to the blade design. The first sort of approximations give rise to blade-to-blade methods since the calculations are done in the blade-to-blade plane. These methods are popular among designers of axial turbomachinery, but it did not attract much attention among designers of radial turbomachinery. The reason may be connected to the fact that the flow passages are more complicated and there are significant changes in radius.

The other way of tackling the solution consists of working in the hub-to-shroud plane (i.e. in the meridional plane), giving rise to what we could call hub-to-shroud (or through-flow) methods. In this sort of approach, the flow is supposed to be axisymmetric, an approximation that can be interpreted as giving the mean flow through the turbomachine. This sort of approach seems more popular among radial turbomachinery designers. In fact, one can find examples of this kind of procedure as early as 1955, when Smith and Hamrick[3] described some work applied to the redesign of a centrifugal compressor, using a hub-to-shroud method. In this instance the blade shape was kept fixed and given as input, while the shroud contour was altered and evolved as a result of the calculations. The centrifugal compressors described by Smith and Hamrick[3] were built and tested, the experimental results being presented by Osborn *et al.*[4] The experimental results show that this technique produced significant improvements in the overall efficiency and peak pressure ratio.

A different strategy was followed by Jansen and Kirschner,[5] who again described the application of an inverse technique to the design of centrifugal compressors. Contrary to the previous example, the meridional geometry (hub and shroud contours) of the machine is supposed known and given as input. The other inputs consist of a suitable normal blade thickness and the desired velocity loading (difference in velocity across the blade) at hub, mid-span and shroud as a function of distance along the camberline. As a result of the calculations, the blade shape was obtained. This paper presents some experimental evidence suggesting that the procedure gives reliable results when the flow is attached.

The method proposed in the present work has got some similarities to that of Jansen and Kirschner[5] in the sense that it is also a hub-to-shroud inverse technique that assumes the meridional geometry to be known and calculates the blade shape that will satisfy some flow-field conditions, given as input to the procedure. The input design specification used here is a mean swirl (radius times mean tangential velocity $r\bar{V}_\theta$) distribution given throughout the meridional section. This design specification is somewhat unusual, but a suggestion in this direction can already be found in the work of Wu,[6] and it is ideally suited to the design of radial turbomachinery as discussed in Reference 7. In fact, the work of Borges,[7] which presents a three-dimensional inverse method using a mean swirl specification, shows that the mean swirl specification is related to the way the work is imparted to the fluid as it passes through the blade row. In other words, the mean swirl can be related to the blade loading across the blades. Reference 8 also discusses the use of a mean swirl imposition and derives the equations to be used in the present work. Nevertheless, Reference 8 does not present any practical examples of application of the equations.

2. DESCRIPTION OF THE DESIGN METHOD

Throughout this work we will use a right-handed cylindrical polar co-ordinate system defined by (r, θ, z), where r is the radius, θ the angular co-ordinate and z is the axial distance. In addition, we will use an auxiliary co-ordinate α, defined by

$$\alpha = \theta - f(r, z), \tag{1}$$

where $f(r, z)$ is the angular co-ordinate of a point on the blade camber surface. This variable α can

be interpreted as a sort of helical angular co-ordinate aligned with the blade, so that when

$$\alpha = m\frac{2\pi}{B}, \tag{2}$$

with m an integer ($m = \ldots, -1, 0, 1, 2, 3, \ldots$) and B equal to the number of blades of the turbomachine, we are on a blade surface (equation (2) describes the blade shape).

2.1. *Velocity flow field*

Since it was intended to apply this method to design pumps, it was assumed that the fluid was inviscid and incompressible and, for simplicity, the blade thickness is not considered in this procedure.

In agreement with the through-flow approximation, the flow through the turbomachine will be assumed axisymmetric even in the blade region. This mean velocity field will be calculated using the streamfunction concept and the value of the mean vorticity. Indeed, since the vorticity field is solenoidal, it can be written as the cross product of two gradients of scalar functions. One of these scalar functions may be α according to the fact that all the vorticity is confined to the blades. In fact, if we suppose the far upstream velocity is uniform (an approximation quite frequent), we can say the flow is irrotational at inlet. Concentrating in designs that execute constant work along the span, it is concluded that the flow must remain everywhere irrotational according to Kelvin's theorem. So, if there is any vorticity at all, it must be bound to the blade surfaces, justifying the statement just made. The other scalar function in the expression for the vorticity turns out to be the mean swirl as is shown in Borges.[7] Therefore, the expression for the mean vorticity, $\bar{\boldsymbol{\Omega}}$ is

$$\bar{\boldsymbol{\Omega}} = \nabla r\bar{V}_\theta \times \nabla\alpha \tag{3}$$

and now that the mean vorticity is known, the corresponding velocity field can easily be calculated. It is indeed known that the mean vorticity is the curl of the mean velocity $\bar{\mathbf{V}}$, or

$$\bar{\boldsymbol{\Omega}} = \nabla \times \bar{\mathbf{V}}. \tag{4}$$

Equating the θ-component of equations (3) and (4), the following equation is obtained:

$$\frac{\partial \bar{V}_r}{\partial z} - \frac{\partial \bar{V}_z}{\partial r} = \frac{\partial f}{\partial z}\frac{\partial r\bar{V}_\theta}{\partial r} - \frac{\partial f}{\partial r}\frac{\partial r\bar{V}_\theta}{\partial z} \tag{5}$$

relating the velocity field to the blade shape, f, and the mean swirl $r\bar{V}_\theta$. Besides this equation, the velocity field must satisfy the continuity equation. In order to achieve this we introduce the concept of a streamfunction defined by

$$\bar{V}_r = -\frac{1}{r}\frac{\partial \psi}{\partial z}, \tag{6a}$$

$$\bar{V}_z = \frac{1}{r}\frac{\partial \psi}{\partial r}, \tag{6b}$$

so that this definition satisfies identically the continuity equation for incompressible flow, i.e. $\nabla \cdot \bar{\mathbf{V}} = 0$. The actual value of ψ appearing in definitions (6a) and (6b) is going to be determined substituting (6a) and (6b) in equation (5). In this way we arrive at

$$\frac{\partial^2 \psi}{\partial r^2} - \frac{1}{r}\frac{\partial \psi}{\partial r} + \frac{\partial^2 \psi}{\partial z^2} = -r\left(\frac{\partial f}{\partial z}\frac{\partial r\bar{V}_\theta}{\partial r} - \frac{\partial f}{\partial r}\frac{\partial r\bar{V}_\theta}{\partial z}\right). \tag{7}$$

For the resolution of this equation, it is necessary to specify a complete set of boundary conditions. The boundary condition to use along the endwalls (hub and shroud) is the one that states that there is no flow through the solid walls. Using the streamfunction concept, this fact is expressed as

$$\psi = \text{Const.} \tag{8}$$

or, in other words, the hub and shroud must be streamlines of the flow.

Far upstream, we know the mean velocity vector, $\bar{\mathbf{V}}_{-\infty}$, since it is given as input. Therefore we can write

$$\frac{1}{r}\frac{\partial \psi}{\partial s} = \bar{\mathbf{V}}_{-\infty} \cdot \mathbf{n}, \tag{9}$$

where s is distance along the far upstream boundary and $\mathbf{n}$ is the unitary vector perpendicular to it. This expression enables us to calculate the values of ψ along the far upstream boundary, using a simple numerical integration. At the far downstream boundary, a similar expression applies since the velocity there is uniform because the flow is irrotational at inlet and the blade row is supposed to execute constant work along the span. In this way, the complete set of boundary conditions is obtained.

The partial differential equation (7) was solved using finite difference techniques. As a typical mixed-flow pump has a meridional section with complicated geometry bounded by curved boundaries (hub and shroud profiles), it was decided to use a transformation of co-ordinates to body-fitted curvilinear co-ordinates.[9] Since this co-ordinate system should be easy to generate and require little computational time, it was decided to use an algebraic transformation. For this kind of transformation of co-ordinates, mesh points are distributed along quasi-orthogonals and quasi-streamlines. Figure 2 shows the grid used in the calculations to be discussed later on.

Equation (7) was discretized using second-order-accurate central difference formulae, obtaining a nine-point difference star. The resulting finite difference equations were solved by a relaxation method. In the present case, a Gauss–Seidel relaxation scheme was used, implemented in conjunction with a multi-grid technique in order to accelerate the convergence rate of the solution. A good description of multi-grid methods can be found in Reference 10, and, in fact, the relaxation subroutines used in our program are a slightly modified version of the ones presented in Reference 10.

2.2. Equation for the determination of the blade shape

After calculating the velocity field using the information presented in the previous subsection, it is necessary to evaluate the blade geometry. That is done by requiring the blade to be tangent to the velocity vector. This condition can be expressed as

$$\bar{\mathbf{W}} \cdot \nabla \alpha = 0, \tag{10}$$

where $\bar{\mathbf{W}}$ is the local relative velocity, $\bar{\mathbf{W}} = \bar{\mathbf{V}} - \mathbf{U}$. Expanding equation (10), the following expression is obtained:

$$\bar{V}_z \frac{\partial f}{\partial z} + \bar{V}_r \frac{\partial f}{\partial r} = \frac{r\bar{V}_\theta}{r^2} - \omega, \tag{11}$$

where f is the angular co-ordinate of the blade and ω is the rotational speed of the blade row. $\bar{V}_z$ and $\bar{V}_r$ are the mean axial and radial velocities, respectively.

Equation (11) is a first-order partial differential equation with characteristic lines coincident with the meridional projection of the streamlines. In order to integrate this differential equation,

some initial data must be specified along a line roughly perpendicular to these characteristic lines and extending from hub to shroud. This initial data on f will be called the stacking condition of the blade. In our method this stacking condition is implemented by giving, as input, the values of the blade angular co-ordinate f, along a quasi-orthogonal, e.g. at the leading edge.

After the stacking condition is specified, we can integrate equation (11), since all the velocities that appear in it are known from the previous iteration. Integration of equation (11) was done using finite difference methods. More specifically, an Euler's modified method[11] was used. This is an implicit numerical scheme that has a truncation error of second order in the mesh size and is consistent and stable.

For some of the cases considered, namely turbomachines with blades covering a large tangential extent such as the one to be discussed, it was found convenient to use some underelaxation in the process of updating the blade geometry. This was done according to the expression

$$f_{\text{new}} = f_{\text{old}} + \text{RF} * (f_{\text{new}} - f_{\text{old}}), \tag{12}$$

where RF is the relaxation factor, f_{new} is the new blade co-ordinate, solution of equation (11), and f_{old} is the blade co-ordinate used in the last iteration.

2.3. *Estimation of blade surface pressures*

One result that is important in any design method is the value of pressure on the suction and pressure surfaces of the blade, for judging whether the pressure distribution is adequate or not. In order to calculate these values starting from the axisymmetric solution, it is necessary to estimate the blade surface velocities using the mean values known. To do this we begin by determining the velocity jump across the blades ($\mathbf{W}^+ - \mathbf{W}^-$) which is given by[7]

$$\mathbf{W}^+ - \mathbf{W}^- = \frac{2\pi}{B} \frac{(\nabla r \bar{V}_\theta \times \nabla\alpha) \times \nabla\alpha}{\nabla\alpha \cdot \nabla\alpha}, \tag{13}$$

where, for a pump, $\mathbf{W}^+$ is the relative velocity at the pressure surface and $\mathbf{W}^-$ is the relative velocity at the suction surface. This expression is physically plausible as it gives a jump in velocity which lies on the blade since it is normal to $\nabla\alpha$ (a vector itself normal to the blade). In addition, we would expect the jump to be normal to the vorticity vector, $(2\pi/B)(\nabla r \bar{V}_\theta \times \nabla\alpha)$, lying in the blade. Knowing the velocity jump and assuming the velocity profile is linear between suction and pressure surfaces (a frequent approximation in hub-to-shroud methods, see Reference 12) it is possible to estimate the velocities at the suction and pressure surfaces. Indeed, their values are going to be equal to the mean velocity (solution of the axisymmetric problem) plus or minus one-half the velocity jump. Afterwards, using the fact that the flow is irrotational at inlet and applying Bernoulli's equation, the expression for the difference in pressure across the blades is obtained. The final expression is[7]

$$p^+ - p^- = \frac{2\pi}{B} \rho \bar{\mathbf{W}} \cdot \nabla r \bar{V}_\theta \tag{14}$$

where p^+ is the pressure at the pressure surface, p^- the pressure at the suction surface and ρ is the fluid density. $\bar{\mathbf{W}}$ is known from the velocity field calculation so that all the terms in the right-hand side of equation (14) are known, enabling the estimation of the pressure loading across the blades.

2.4. *Flowchart*

To end Section 2, we would like to draw the attention of the reader to the fact that the vorticity depends on the blade shape, f, which in its turn is an outcome of the calculations. So, the

calculations must be iterated until convergence is obtained. This is done according to the following flowchart:

(i) input of initial data—specified values of $r\bar{V}_\theta$, definition of meridional section and body-fitted curvilinear co-ordinate system and all the relevant parameters;
(ii) estimation of a first guess for f, assuming that the mean velocity is uniform along the quasi-orthogonals;
(iii) using the input values of mean swirl, $r\bar{V}_\theta$, and the values of blade shape, f, from last iteration, calculate the mean velocity field (solution of equation (7));
(iv) update the blade shape, f, by integration of equation (11) and using underelaxation as defined in equation (12);
(v) if the solution is converged output the blade shape, f, and other relevant results. Otherwise go back to step (iii) and initiate a new iteration.

This flowchart was implemented as a FORTRAN computer code and applied to the design of the impeller of a mixed-flow pump.

3. DISCUSSION OF APPLICATION TO A MIXED-FLOW PUMP

In order to show the potentialities of the method, it was decided to apply it to the design of a mixed-flow pump. The chosen pump was based on a real machine which had as nominal conditions, a value of 28 m for the head, H, a nominal volume flow, Q, of 600 m^3/h and a rotational speed of 1450 rpm. These values give a non-dimensional specific speed parameter equal to 0·919. The rotor has eight blades and a tip diameter equal to 320 mm. This value will be used to non-dimensionalize all the linear dimensions and the velocities will be made non-dimensional by using the transport blade-tip velocity, ωr_{tip} (its value is 24·3 m/s).

The meridional geometry used in the calculations is based on an existing pump (with minor alterations), designed by a Portuguese pump manufacturer using hand calculations and graphical processes. The final meridional shape used is defined in Figure 1. A grid formed by 145 quasi-orthogonals and 57 quasi-streamlines was fitted to this meridional section, there being in the blade region, a total of 61 × 57 points. Figure 2 shows every other line of the grid used. As can be seen, a region upstream and downstream of the blade zone was considered in the calculations.

An important input to the present inverse method is the specification of mean swirl, $r\bar{V}_\theta$. As it is supposed that the pump accepts the flow with no swirl, the value of $r\bar{V}_\theta$ along the entire leading edge is considered equal to zero. At the trailing edge the value was also considered constant in order to obtain a design that executes constant work along the span. The necessary value of $r\bar{V}_\theta$ at the trailing edge depends on the work transfer per unit mass of fluid desired for the rotor, which is a value determined by the desired head and an assumed value of efficiency (in our case considered equal to 0·86). The value of $r\bar{V}_\theta$ used at the trailing edge is 0·5411 ωr_{tip}^2.

Another restriction was imposed on the derivatives of the mean swirl at the leading and trailing edges, namely, we forced there a zero derivative along the quasi-streamlines. This was done in order to obtain a zero pressure loading at the trailing edge (as is required by the Kutta–Joukowski condition), and at the leading edge. The equivalence between a zero derivative of the mean swirl and zero pressure loading can be seen from expression (14) which shows that the pressure loading depends on the gradient of mean swirl, being zero where the gradient of $r\bar{V}_\theta$ is zero, as it is the case at the leading and trailing edges.

This close equivalence between derivatives of mean swirl and pressure loading across the blade was one of the factors used when choosing the input mean swirl, $r\bar{V}_\theta$, along the entire meridional section, and whose contours are presented in Figure 3. The other factor considered was the

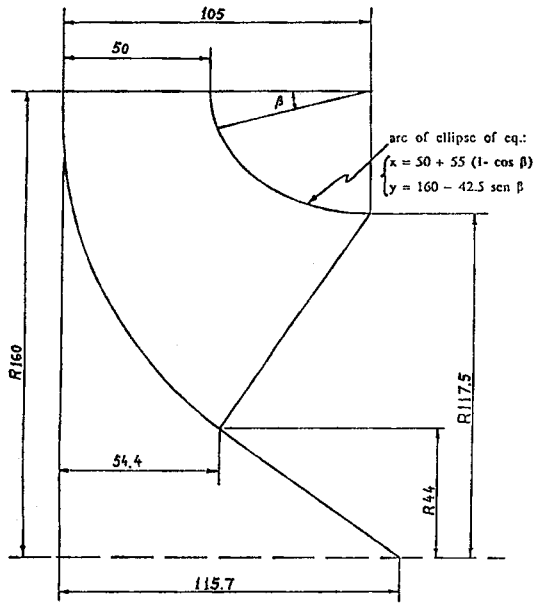

Figure 1. Definition of meridional geometry (dimensions in mm)

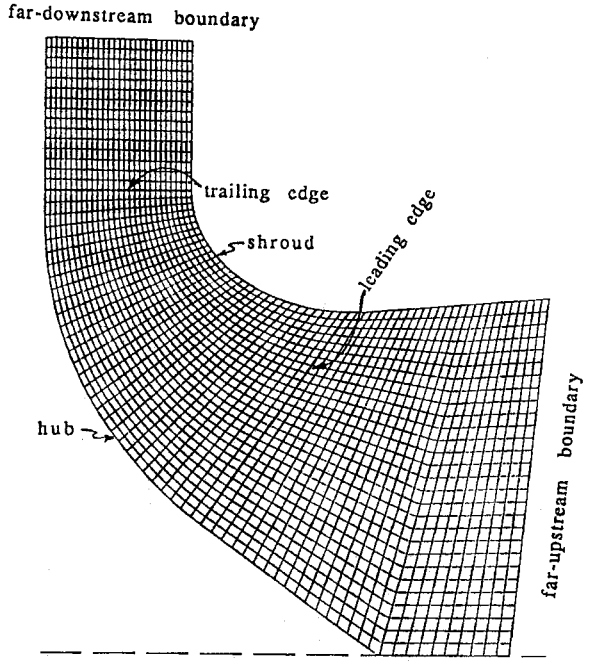

Figure 2. Grid used in the meridional plane

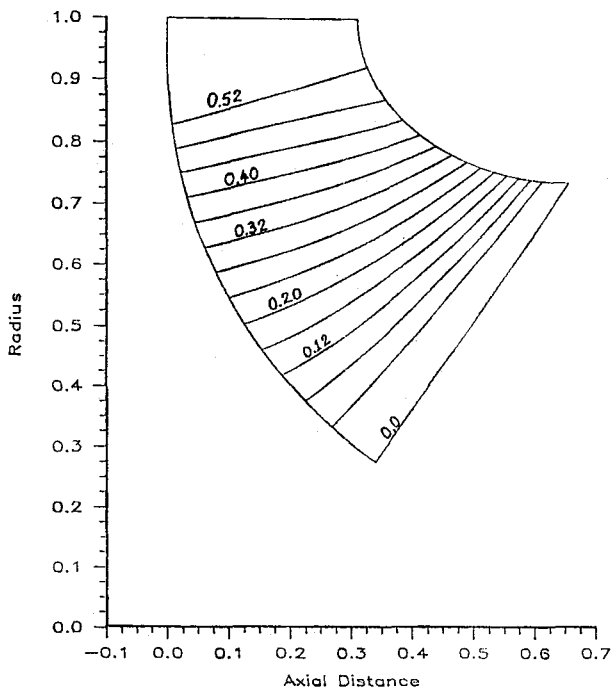

Figure 3. Contours of the input mean-swirl distribution (defined as $r\bar{V}_\theta/(r_{tip}U_{tip})$)

attempt to avoid a blade shape too twisted which would be difficult to manufacture. These two factors were exactly the same guidelines advanced and discussed in Reference 7 when choosing the mean swirl for a completely different turbomachine, a radial inflow turbine.

Recalling briefly the arguments advanced in Reference 7 and which are sufficiently general to apply to the present situation, it is evident from expression (14) that the pressure blade loading is proportional to the product of the modulus of the relative velocity and the value of the derivative of $r\bar{V}_\theta$ along the meridional projection of the flow streamlines, or

$$p^+ - p^- = \frac{2\pi}{B}\rho|\bar{\mathbf{W}}_m|\frac{\partial r\bar{V}_\theta}{\partial m}, \tag{15}$$

where $|\bar{\mathbf{W}}_m|$ is the modulus of the meridional projection of the relative velocity and m is distance along the meridional projection of the streamlines. In a well designed machine, $|\bar{\mathbf{W}}_m|$ does not vary abruptly and the streamlines have a direction close to the quasi-streamlines. Therefore, equation (15) implies that the pressure blade loading is mainly influenced by the value of the derivative of $r\bar{V}_\theta$ along the quasi-streamlines, which is a value known at the start of the calculations, and so can be controlled. In this way, if it is desired to design a blade with a big loading near the leading edge, then the derivatives of $r\bar{V}_\theta$ along the quasi-streamlines should have large values near the leading edge. In addition, if one wishes to obtain a pressure loading with a smooth evolution, then the derivatives of $r\bar{V}_\theta$ should be watched with special care, specifying them with a variation from the leading to the trailing edge as gradual and smooth as possible. From the point of view of the pressure loading, the most unfavourable situation is along the shroud where the velocities and decelerations are higher, so that the derivatives there should have a smooth variation.

The other argument that one should bear in mind when choosing the input mean swirl schedule is the one connected with the amount of blade twist. In order to clearly understand this argument it is important to rewrite equation (11) along the meridional projection of a streamline, obtaining

$$f_a - f_b = \int_b^a \frac{\bar{W}_\theta}{r\bar{V}_m}\,dm = \int_b^a \frac{(\bar{V}_\theta - \omega r)}{r\bar{V}_m}\,dm, \tag{16}$$

where a and b are two arbitrary points on the same streamline, f is the angular co-ordinate of the blade, $\bar{V}_m$ is the mean velocity in the meridional plane and m is the distance along the meridional projection of the streamline. If one wishes to control the total variation in the angular co-ordinate of the blade, $f_a - f_b$, it is convenient to avoid high values for the expression under the integral sign in equation (16). This can be achieved if one specifies the value of $r\bar{V}_\theta$ so that $\bar{W}_\theta$ has small values, or in other words, if one specifies $r\bar{V}_\theta$ so that the value of $\bar{V}_\theta$ closely follows the local value of the transport velocity, ωr. Taking note that $\bar{W}_\theta$ is divided by $r\bar{V}_m$ in the integrand of equation (16), one can conclude that the use of small values for $\bar{W}_\theta$ is more important and critical where the radius and the meridional velocity $\bar{V}_m$ present smaller values. So, from the point of view of highly twisted blades, the most critical streamsurface is the hub, not only because there the radius and meridional velocity take the lower values in the machine, but also because the meridional flow path is usually longer along the hub than anywhere else in the machine.

The next set of four figures is presented to demonstrate that the above two points were taken into consideration. Indeed, Figure 4 gives the evolution of the input $r\bar{V}_\theta$ on the hub and the shroud. It is clearly seen that on the shroud the evolution of $r\bar{V}_\theta$ is quite gradual and smooth, while at the hub the opposite happens.

Figure 5 shows, on the same graph, the values of ωr and the specified values $\bar{V}_\theta$ at the hub. Here it is evident that, on the hub, $\bar{V}_\theta$ has an evolution which is almost parallel to ωr, for most of the flow path and without much consideration in the direction of obtaining smooth derivatives. This

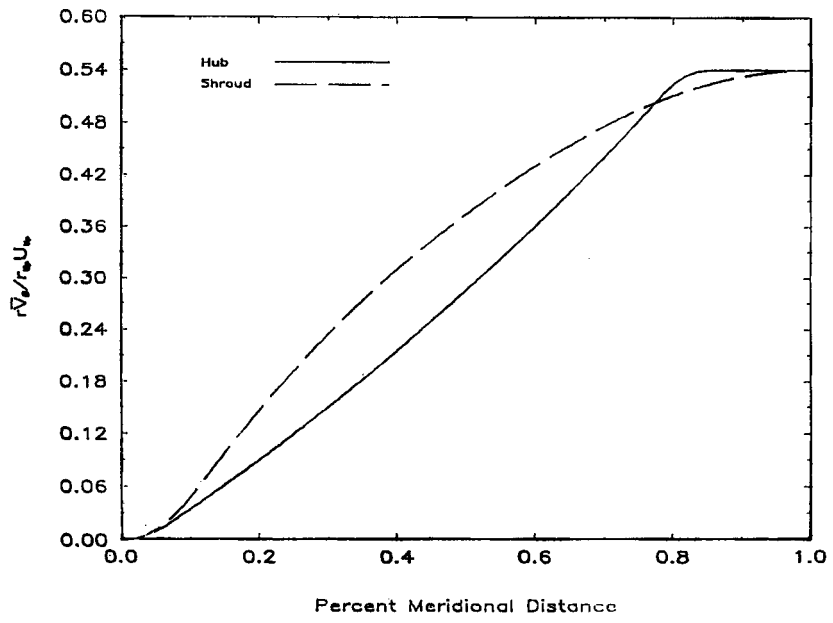

Figure 4. Input mean swirl distribution at hub and shroud

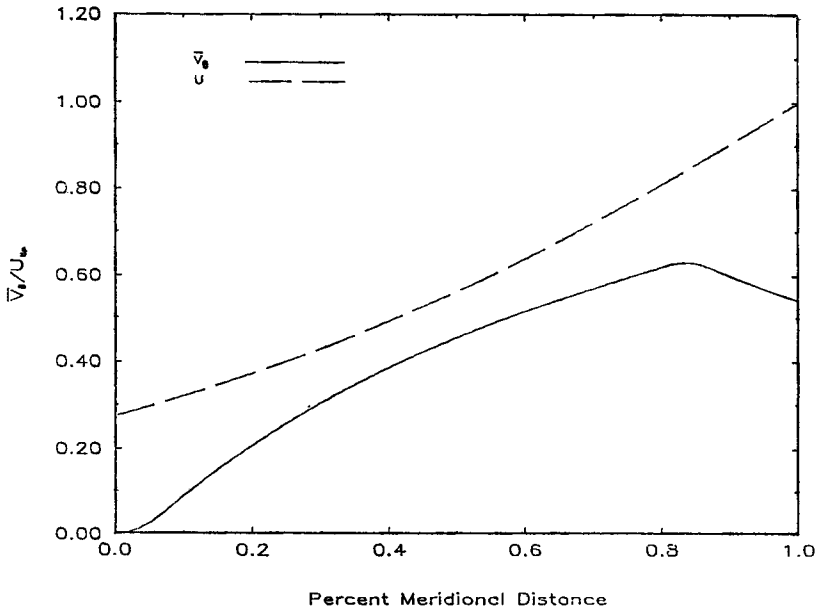

Figure 5. Mean tangential velocity and blade speed at hub

was done so that $\bar{W}_\theta$ at the hub presented small and approximately constant values along most of the blade, leading to a reasonable overall change in the values of blade angular co-ordinate, f.

From Figure 6, it can be seen that the contrary happens on the shroud, where $\bar{V}_\theta$ was chosen to have a smooth variation rather than following the local value of blade speed, ωr. In fact, the main concern when specifying the mean swirl at the shroud was to obtain an adequate pressure distribution and not to control the overall variation in the blade angular co-ordinate, f.

The above ideas are corroborated by Figure 7, where the derivatives of $r\bar{V}_\theta$ along the quasi-streamlines for the hub and the shroud are presented. As can be clearly seen, the derivatives at the shroud present a smooth variation while the same does not apply at the hub, where a more abrupt change of the $r\bar{V}_\theta$ derivatives can be detected.

Using the close relationship between $r\bar{V}_\theta$ derivatives and pressure loading, one can conclude that the present design presents a large loading near the leading edge at the shroud streamsurface, while at the hub streamsurface, the blade loading is more evenly spread. However, one should point out that, at the hub, the derivative is zero for approximately the last 15% of the meridional flow path. This indicates that there will be a small pressure loading along the last portion of the blade at the hub, suggesting that perhaps one could use a shorter flow path there. This idea would entail an alteration of the trailing edge shape (using a trailing edge inclined to the axis, instead of parallel) and so, was not pursued further.

The inverse computer code was run, using the input described above together with a stacking condition imposed at the trailing edge and which consists of a linear variation of f between the value of 0·0 rad (at the hub) and 0·10 rad (at the shroud). As a result, the blade shape described in the next figure was obtained. Since it is difficult to visualize the three-dimensional geometry of the blade, it was decided to present the blade geometry in Figure 8 as a view of two consecutive blades, as would be seen by an observer looking in the direction of the impeller axis. The blade

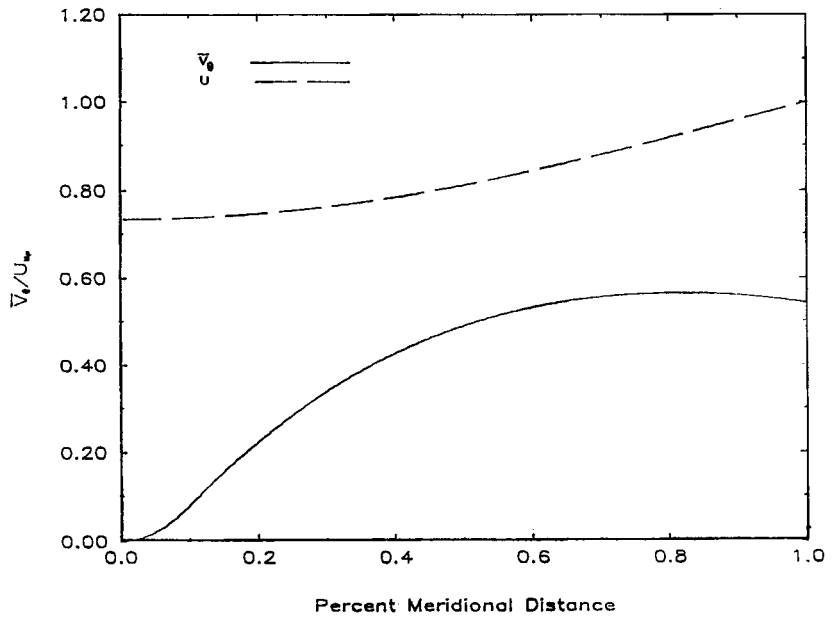

Figure 6. Mean tangential velocity and blade speed at shroud

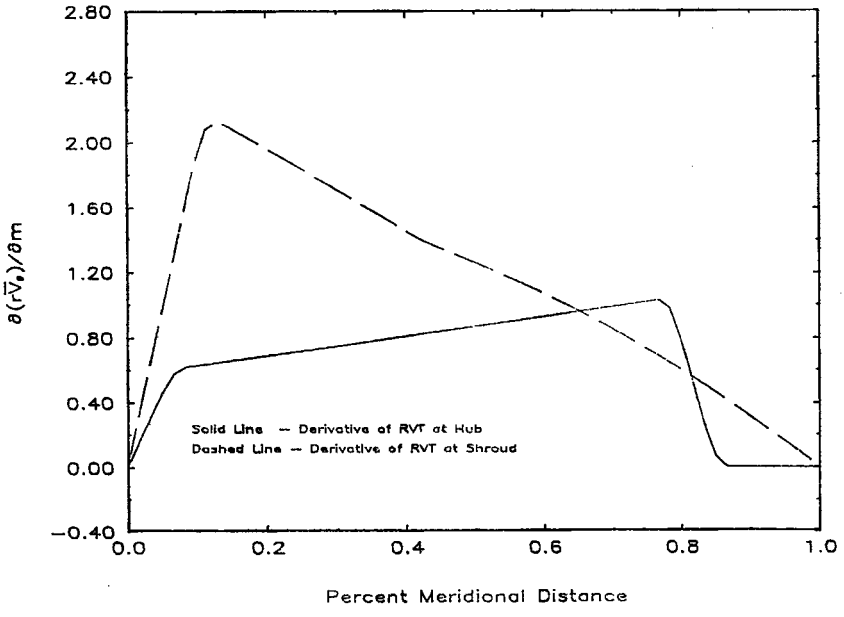

Figure 7. Derivatives of the input mean-swirl distribution

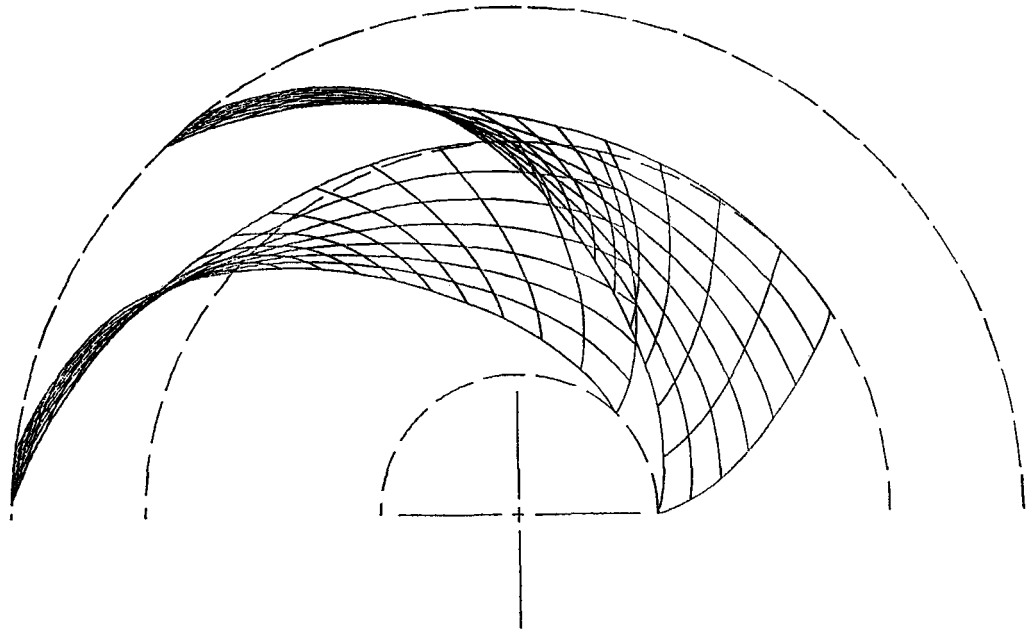

Figure 8. Blade projection along the axis

obtained seems typical of a pump impeller and no particular problems are envisaged during its manufacture, since it is not a highly twisted blade.

Figure 9 presents the estimated pressure distribution on hub and shroud, assuming a linear variation of the velocity from suction to pressure surfaces and using the procedure already discussed in Subsection 2.3. The pressure coefficient, C_p, used in this plot is defined as

$$C_p = \left(\frac{\mathbf{W}}{\mathbf{W}_{ref}}\right)^2 - 1, \tag{17}$$

where $\mathbf{W}_{ref}$ is a reference relative velocity, which is equal to 0·308 ωr_{tip} in the present case. Note that the loading has a behaviour similar to the evolution of the derivatives of $r\bar{V}_\theta$ along the quasi-streamlines, shown in Figure 7, bearing out the comments made above, concerning the close relationship between derivatives of $r\bar{V}_\theta$ and pressure loading. For example, it is seen that, at the hub, the pressure loading varies more abruptly than at the shroud, and along the last 15% of the flow path at the hub, the pressure loading is zero as was already expected from the values of the derivatives of mean swirl. It should also be remarked that the distribution of pressure on the blade surfaces at the hub is not ideal since its variation is not smooth and presents some unnecessary decelerations. However, the optimization of the pressure distribution would entail changes in the meridional section of the machine, and so was not tried in this work.

The evolution of the maximum absolute error in the blade angular co-ordinate, f, between two successive iterations, as a function of the iteration number is given in Figure 10 for the present case where a relaxation factor varying between 0·5 and 0·15 was used. It is seen that the convergence is fairly rapid requiring 45 iterations, and is monotonic for the most part.

As already mentioned, each global iteration required the evaluation of the mean velocity field and blade shape. The most demanding task between these two calculations is the determination

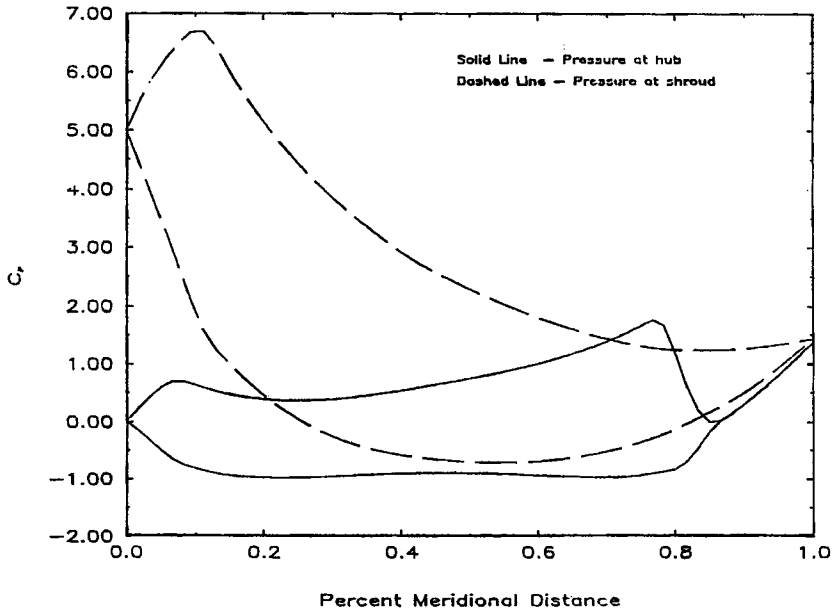

Figure 9. Pressure distribution at hub and shroud

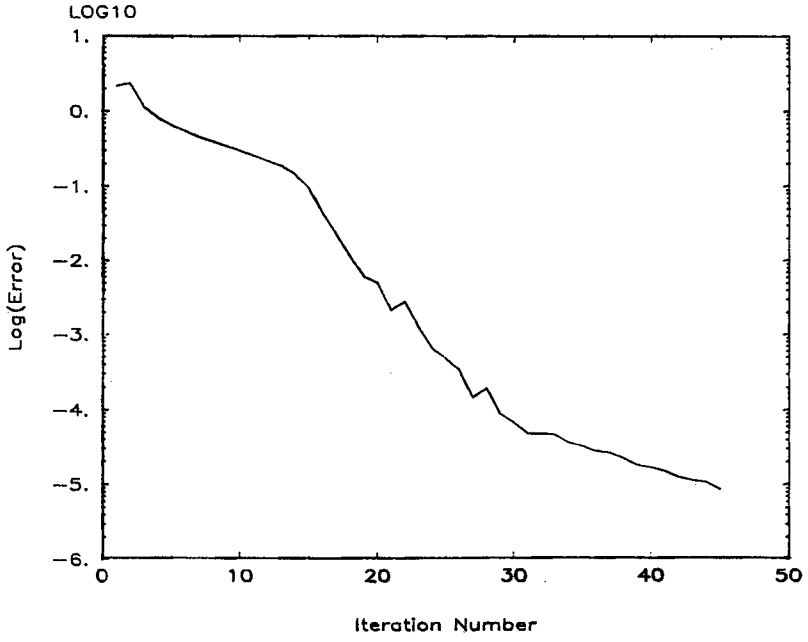

Figure 10. Convergence history of the maximum absolute error in the blade angular co-ordinate, f

of the velocity field. For the case being discussed, the amount of computational work required for the solution of the velocity field (solution of equation (7), using a relaxation method as described in Subsection 2.1) is roughly equivalent to 28 Gauss–Seidel sweeps, during the first few global iterations. This amount of work decreased steadily as the computation evolved since the results from the previous mean velocity field calculation were used as an initial approximation in the following iteration, providing an increasingly accurate first approximation as convergence is achieved.

In order to study the influence of the grid size, this example was run using a finer and coarser mesh. The finer grid is defined by 289 quasi-orthogonals and 113 quasi-streamlines, while the coarser grid has 73 quasi-orthogonals by 29 quasi-streamlines. The size of the grids was chosen so that the number of quasi-streamlines and quasi-orthogonals was doubled twice, first as one moves from the coarser grid (73×29) to the standard mesh (145×57) and then again as one goes from the standard grid to the finer one (289×113). The results showed a maximum absolute difference in the blade angular co-ordinate, f, between the coarser and standard grids equal to $5{\cdot}65 \times 10^{-3}$ rad, while same difference between the standard and finer mesh was reduced to $1{\cdot}37 \times 10^{-3}$ rad. Bearing in mind that the overall variation in the blade angular co-ordinate is approximately 2·32 rad, it is seen that the differences between the results obtained with the three grids are very small. In fact, these differences are so small that they cannot be distinguished in a plot comparing the blade shapes computed with the different grids. Therefore, instead of presenting such a plot, it was decided to compare the estimated pressure distributions calculated with the three grids, in Figure 11. It is clearly seen that the variations between the grids are quite small and confined to regions where there is a sudden change of blade pressure loading. Based upon these results it is concluded that, for the standard grid used in the present study, the results depend little on the grid size.

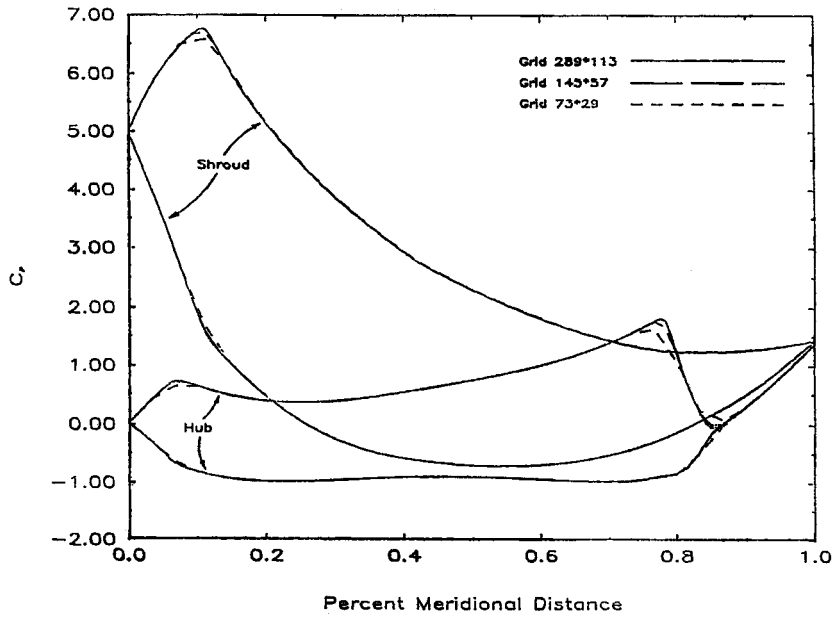

Figure 11. Comparison of results obtained with the different grids

One advantage of the present method lies in the fact that it is quite rapid, requiring small amounts of CPU time. In fact, the present run required 1 min 57 s of CPU time in a VAX 3400 computer, including the pre-processing phase. Since it is computationally so cheap, several different input mean swirl distributions can be scanned quickly, enabling the choice of the most appropriate mean swirl schedule.

A second example of blade design, using a mean swirl distribution chosen among the several input $r\bar{V}_\theta$ distributions scanned, will be presented in the following, in order to clarify the close relationship between the mean swirl specification and the results for the blade shape and pressure distribution.

The input mean swirl distribution used in this second run is defined in Figure 12, which shows the specified $r\bar{V}_\theta$ values at hub and shroud, and in Figure 13 which gives the evolution of the derivatives of $r\bar{V}_\theta$ along the quasi-streamlines at hub and shroud. These plots should be compared with the corresponding figures for the first example, which are presented as Figures 4 and 7, respectively. This comparison indicates that this second $r\bar{V}_\theta$ distribution has a more gradual variation than the previous input mean swirl, especially at the hub. In fact, this case does not show a region where the values of $r\bar{V}_\theta$ are constant or, in other words, where the $r\bar{V}_\theta$ derivatives are zero, as the previous case showed near the trailing edge. Another difference at hub lies in the fact that this second example has the region with higher derivatives closer to the leading edge which is exactly the opposite to what happened in the first example. At the shroud, the overall evolution of the mean swirl schedule is similar in both cases. However, the maximum values of the $r\bar{V}_\theta$ derivatives are smaller, both at shroud and hub, for the second distribution being considered.

Some of the results obtained with this mean swirl specification, maintaining all the other inputs equal, are displayed in Figure 14 which presents the blade shape, and in Figure 15 which shows the estimated blade pressure distributions at hub and shroud. These two graphs should be compared with the corresponding plots for the first run, which are presented as Figures 8 and 9, respectively.

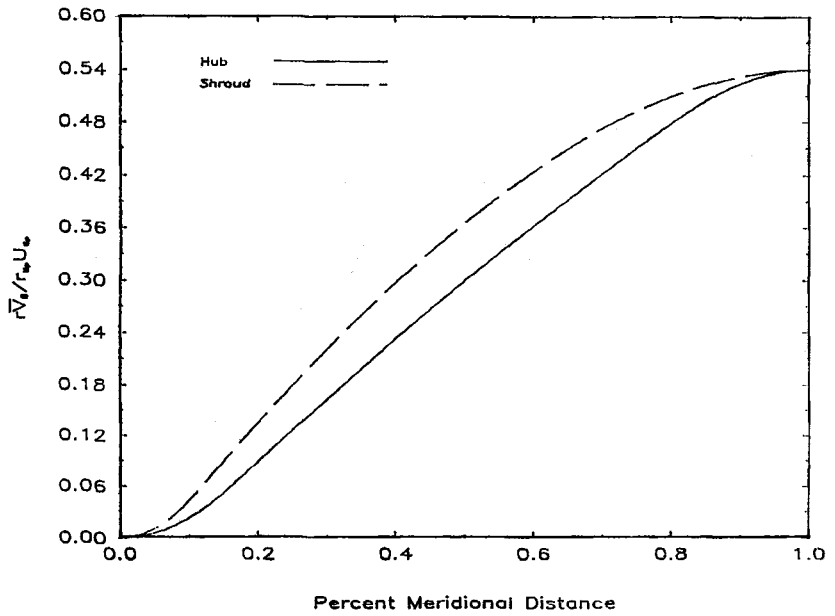

Figure 12. Input mean swirl distribution at hub and shroud (second example)

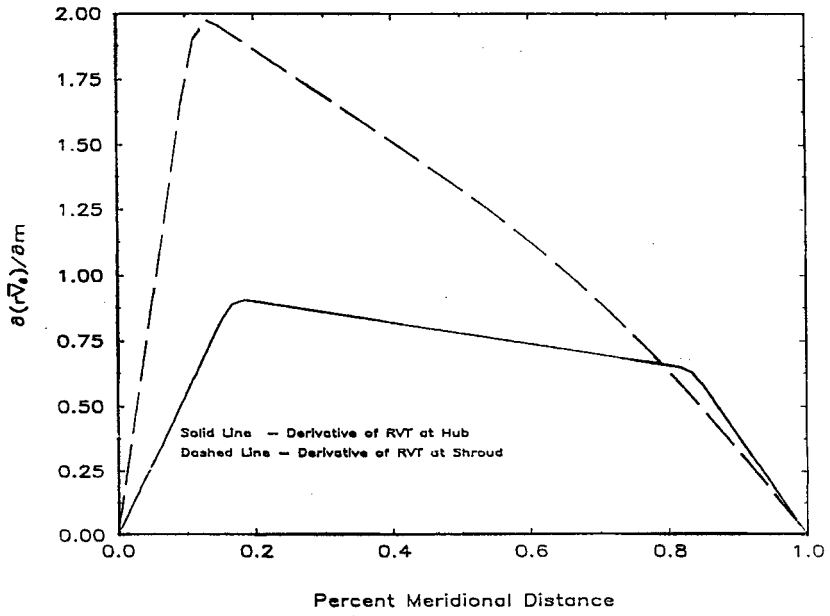

Figure 13. Derivatives of the input mean-swirl distribution (second example)

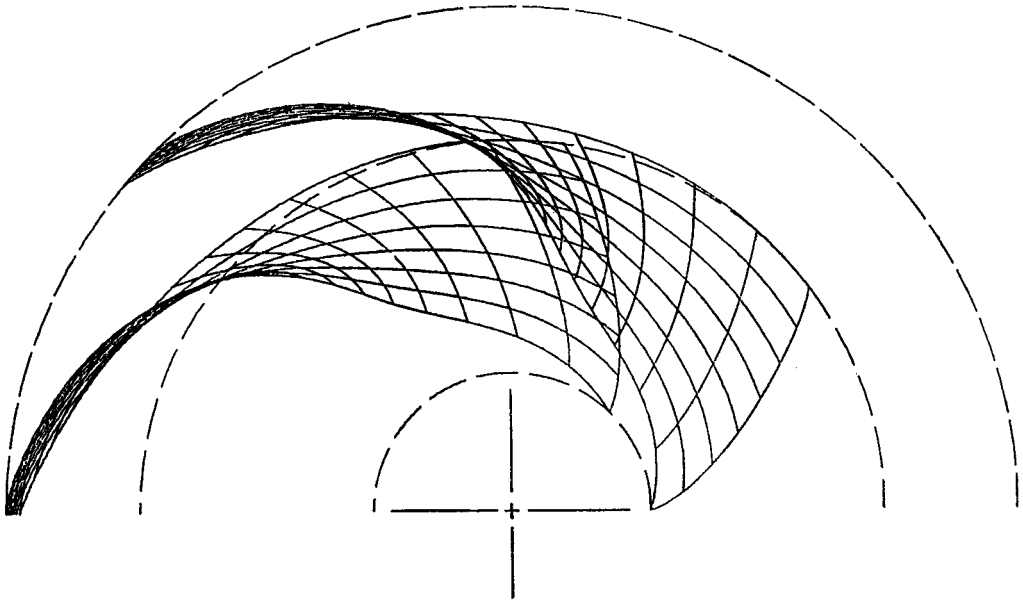

Figure 14. Blade projection along the axis (second example)

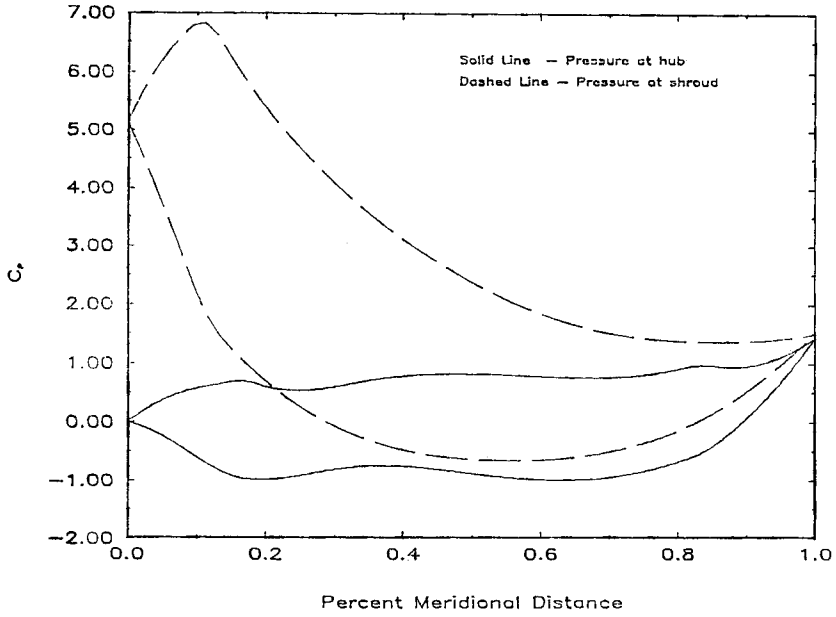

Figure 15. Pressure distribution at hub and shroud (second example)

It can be seen in Figure 14 that the overall variation in blade co-ordinate angle is greater for this last case, taking the value of 2·44 rad instead of 2·32 rad for the first example. In addition, the blade being discussed presents a more twisted shape. Due to the conjunction of these two aspects, it is believed that this last blade would be more difficult to manufacture accurately than the other one. It should also be remarked that this example serves to demonstrate that a smoother $r\bar{V}_\theta$ distribution does not inevitably lead to a less twisted blade.

The figure with the estimated blade pressure distributions shows that the blade pressure loading has again an overall evolution analogous to the one displayed by the $r\bar{V}_\theta$ derivatives. Comparing this result with the blade pressure distribution for the first example, it is seen that the biggest differences are found at hub, as one would expect from the fact that the more pronounced changes in the $r\bar{V}_\theta$ derivatives were introduced at hub. Note also that this last design shows a more uniform blade pressure loading than the first example which had a zone of higher loading towards the end of the blade, at the hub.

4. CONCLUSIONS

A through-flow (hub-to-shroud) inverse method was proposed and implemented as a computer code. In the present implementation, the flow is assumed incompressible, irrotational at inlet and the blade thickness was not considered during the calculations. The necessary equations are presented and, as an example of a possible application, the inverse method was used to redesign the rotor of a mixed-flow pump.

The present method uses as an input specification the value of mean swirl, $r\bar{V}_\theta$. This input specification was chosen using a reasoning similar to that used in Reference 7. This is remarkable, since the turbomachine designed in Reference 7 was a radial-inflow turbine, and indicates that the strategy developed there is quite general, being able to cope with radically different machines.

Briefly, this strategy consists in using the input mean swirl to control the pressure loading on the blades and the overall variation in the angular co-ordinate of the blade, f.

One advantage of the present technique is the fact that it requires small amounts of CPU time. So it is a convenient tool to scan quickly and inexpensively several different input mean swirl distributions, in order to find the most appropriate one. The results for two different input $r\bar{V}_\theta$ specifications are presented.

This work also shows that further research should be done in order to obtain reasonable pressure distributions on the blade surfaces. In fact, the designs presented here have pressure distributions on the hub which are not the ideal ones. The optimization of the pressure distribution will probably involve some changes in the meridional section (hub and shroud contours).

ACKNOWLEDGEMENTS

The work described here was financially supported by CTAMFUTL/INIC. The suggestions and help of the technical staff of EFACEC are also gratefully acknowledged.

REFERENCES

1. S. Lazarkiewicz and A. T. Troskolanski, *Impeller Pumps*, Pergamon Press, Oxford, 1965.
2. V. S. Lobanoff and R. R. Ross, *Centrifugal Pumps: Design & Application*. Chap. 3, Gulf Publishing Company, Houston, Texas, 1985, pp. 28–45.
3. K. J. Smith and J. T. Hamrick, 'A rapid approximate method for the design of hub shroud profiles of centrifugal impellers of given blade shape', *NACA Technical Note 3399*, 1955.
4. W. M. Osborn, K. J. Smith and J. T. Hamrick, 'Design and test of mixed-flow impellers VIII—comparison of experimental results for three impellers with shroud redesigned by rapid approximate method', *NACA Research Memorandum E56L07*, 1957.
5. W. Jansen and A. M. Kirschner, 'Impeller blade design method for centrifugal compressors', *NASA SP304, Part 2*, 1974, pp. 537–563.
6. C. -H. Wu, 'A general theory of three-dimensional flow in subsonic and supersonic turbomachines of axial-, radial- and mixed-flow types', *NACA Technical Note 2604*, January 1952.
7. J. E. Borges, 'A three-dimensional inverse method for turbomachinery: Part I—Theory', *Trans. ASME, J. Turbomachinery*, **112**(3), 346–354 (1990).
8. W. R. Hawthorne, 'The actuator duct representation of turbomachinery blade rows, *CUED/A-Turbo/TR 119*, 1983.
9. J. F. Thompson, Z. U. A. Warsi and C. W. Mastin, 'Boundary-fitted curvilinear coordinate systems for solution of partial differential equations—A review', *J. Comput. Phys.*, **47**, 1–108 (1982).
10. A. Brandt, 'Multi-level adaptive solutions to boundary-value problems', *Math. Comput.*, **31**(138), 333–390 (1977).
11. P. J. Roache, *Computational Fluid Dynamics*, Hermosa Publishers, Albuquerque, N.M., U.S.A., 1982, pp. 84–85.
12. J. D. Stanitz and V. D. Prian, 'A rapid approximate method for determining velocity distribution on impeller blades of centrifugal compressors', *NACA Technical Note 2421*, 1951.